PASJ: Publ. Astron. Soc. Japan **59**, 889–895, 2007 October 25

Astrometry of Galactic Star-Forming Region Sharpless 269 with VERA: Parallax Measurements and Constraint on Outer Rotation Curve

Mareki HONMA,[1,2] Takeshi BUSHIMATA,[1,3] Yoon Kyung CHOI,[1,4] Tomoya HIROTA,[1] Hiroshi IMAI,[5] Kenzaburo IWADATE,[6] Takaaki JIKE,[6] Osamu KAMEYA,[2,6] Ryuichi KAMOHARA,[1] Yukitoshi KAN-YA,[1,7] Noriyuki KAWAGUCHI,[1,2] Masachika KIJIMA,[1,2] Hideyuki KOBAYASHI,[1,3,4,6] Seisuke KUJI,[6] Tomoharu KURAYAMA,[1] Seiji MANABE,[2,6] Takeshi MIYAJI,[1,3] Takumi NAGAYAMA,[5] Akiharu NAKAGAWA,[5] Chung Sik OH,[1,4] Toshihiro OMODAKA,[5] Tomoaki OYAMA,[1] Satoshi SAKAI,[6] Katsuhisa SATO,[6] Tetsuo SASAO,[8,9] Katsunori M. SHIBATA,[1,3] Motonobu SHINTANI,[5] Hiroshi SUDA,[4,6] Yoshiaki TAMURA,[2,6] Miyuki TSUSHIMA,[5] and Kazuyoshi YAMASHITA[1,2]

[1]*Mizusawa VERA Observatory, National Astronomical Observatory, 2-21-1 Osawa, Mitaka, Tokyo 181-8588*

[2]*Graduate University for Advanced Studies, 2-21-1 Osawa, Mitaka, Tokyo 181-8588*

[3]*Space VLBI Project, National Astronomical Observatory, 2-21-1 Osawa, Mitaka, Tokyo 181-8588*

[4]*Department of Astronomy, The University of Tokyo, 7-3-1 Hongo, Bunkyo, Tokyo 113-8654*

[5]*Faculty of Science, Kagoshima University, 1-21-35 Korimoto, Kagoshima 890-0065*

[6]*Mizusawa VERA observatory, National Astronomical Observatory of Japan, Mizusawa, Oshu, Iwate 023-0861*

[7]*Department of Astronomy, Yonsei University, Seoul 120-749, Republic of Korea*

[8]*Ajou University, Suwon 442-749, Republic of Korea*

[9]*Korean VLBI Network, KASI, Seoul 120-749, Republic of Korea*

honmamr@cc.nao.ac.jp

(Received 2007 March 9; accepted 2007 May 20)

Abstract

We have performed high-precision astrometry of H_2O maser sources in the Galactic star-forming region Sharpless 269 (S269) with VERA. We successfully detected a trigonometric parallax of 189 ± 8 μas, corresponding to a source distance of $5.28^{+0.24}_{-0.22}$ kpc. This is the smallest parallax ever measured, and the first one detected beyond 5 kpc. The source distance as well as the proper motions were used to constrain the outer rotation curve of the Galaxy, demonstrating that the difference of rotation velocities at the Sun and at S269 (which is 13.1 kpc away from the Galaxy's center) is less than 3%. This gives the strongest constraint on the flatness of the outer rotation curve, and provides a direct confirmation of the existence of a large amount of dark matter in the Galaxy's outer disk.

Key words: ISM: star forming regions — ISM: individual (Sharpless 269) — masers (H_2O) — VERA

1. Introduction

Rotation curves, which are plots of rotation velocities as functions of distance from galaxy centers, are important tools to study the mass distributions in disk galaxies. Assuming that the centrifugal force balances with gravity, one can determine the mass distribution in a galaxy using the rotation curve. Observations of rotation curves in external galaxies revealed that they are basically flat within (and often beyond) optical disks of spiral galaxies (e.g., Rubin et al. 1980; Rubin 1983; Sofue & Rubin 2001). Flat rotation curves observed in external galaxies have provided strong evidence for the dark matter in the outer regions of galaxies (e.g., Kent 1986, 1987).

In contrast, the rotation curve of the Milky Way Galaxy remains highly uncertain, particularly in the outer region, although a large number of efforts have been made to determine it (e.g., Clemens 1985; Merrifield 1992; Brand & Blitz 1993; Honma & Sofue 1997, and references therein). The reason for this is twofold: 1) it has been difficult to measure accurate distances of the Galactic objects that are used to trace the rotation curve, such as OB stars and molecular clouds, and 2) in most cases it has been difficult to measure the proper motions of Galactic objects, and thus only the radial velocity (out of the three components of spatial velocity) could be used to constrain the Galactic rotation. Therefore, the outer rotation curve, and hence the dark-matter distribution, in the Galaxy's disk is still highly uncertain, although it is widely believed that the Galaxy's outer rotation curve is flat, just like those of extra-galaxies.

In order to determine a precise rotation curve of the Galaxy, high-precision astrometry is essential. By measuring the accurate position of a star, one can determine a trigonometric parallax, π, and thus the source distance, as $D = 1/\pi$. In addition, high-precision astrometry also allows us to determine source proper motions (source motions projected onto the sky plane), and thus the 3-dimensional space velocity of the source. Still, accurate astrometric measurements have been made only for sources that are located fairly close to the Sun compared to the Galaxy's size. For instance, the HIPPARCOS mission (Perryman et al. 1997), the most modern satellite dedicated to optical astrometry, has reached distances of $\sim$300 pc by parallax measurements, which is much smaller than the size of the Galaxy (e.g., $\sim$15 kpc for the radius of the Galaxy's disk). Hence, at present the astrometry of the Galaxy still remains an unexplored issue.

Over the next decades, there will be new missions for the

astrometry of the Galaxy that will aim at 10 μas accuracy (e.g., SIM[1], GAIA[2], JASMINE[3]). These will be satellite-type missions with optical/infrared telescopes orbiting the Earth, where the observations can be made free from any disturbance of the atmosphere. At radio wavelengths, high-precision astrometry has been performed with ground-based VLBI (Very Long Baseline Interferometry), a radio interferometer with telescopes separated by $\sim$ 1000 to $\sim$ 10000 km. The advantage of VLBI is that it provides the highest angular resolution among the existing telescopes at any wavelength. While normal VLBI observations directly suffer from fluctuation of the atmosphere (mainly due to the water vapor content in the troposphere), a noble way, which is called 'phase-referencing', has been developed to cancel out the tropospheric fluctuations. In phase-referencing observations, a few sources (one target and one or more reference sources) are observed at nearly the same time by rapidly switching the telescope, and then the relative positions of the target with respect to the reference sources can be measured after correcting for any influence of the troposphere. In fact, recently, the distance of the Galactic star-forming region W3OH was determined with VLBA (Xu et al. 2006, Hachisuka et al. 2006) to solve the long-standing ambiguity of the Perseus arm distance by measuring the source distance at 2 kpc. It has also been shown that the maser emissions from late-type stars (such as Mira variables) can be used to perform kpc-scale astrometry with VLBI (Kurayama et al. 2005). These results strongly demonstrate the promising future of ground-based VLBI for the Galaxy-scale astrometry.

VERA (VLBI Exploration of Radio Astrometry) is a new Japanese VLBI array dedicated to VLBI astrometry (Honma et al. 2000; Kobayashi et al. 2003). A unique feature of the VERA telescopes is the dual-beam receiving system, which allows us to observe simultaneously a target and a reference source within 2.°2. This dual-beam system enables one to cancel out tropospheric fluctuations much more effectively than switching observations with normal, single-beam telescopes (Honma et al. 2003). With a target astrometric accuracy of 10 μas, VERA aims to precisely locate hundreds of maser sources in the Galaxy and to explore their 3D structure and dynamics. The VERA array was constructed by 2002, and regular observations started in the fall of 2003. Here, we present some initial results of high-precision astrometry with VERA toward the Galactic star-forming region S269, which is located in the outer regions ($l = 196.°45$). We report on the determination of the smallest parallax in human history. Our results provide a strong constraint on the flatness of the rotation curve in the outer Galaxy.

2. Observations and Reductions

We observed H_2O masers in the Galactic star-forming region Sharpless 269 (S269) with VERA since 2004 November, and here we present the data of 6 epochs that were obtained with the full 4-station array (Mizusawa, Iriki, Ogasawara, and Ishigaki-jima) under relatively good conditions. The epochs are day of year (DOY) 323 in 2004, DOY 026, 073, 134, 266, and 326 in 2005 (2004 November 18, 2005 January 26, March 14, May 14, September 23, and November 21), spanning $\sim$1 year. At each epoch, the H_2O 6_{16}-5_{23} maser line at a rest frequency of 22.235080 GHz in S269 and a position reference source J0613+1306 were simultaneously observed in a dual-beam mode for nearly 9 hours. The typical on-source integration time was 5 hours for both the target maser and the reference. The reference source, J0613+1306, is one of the ICRF sources (Ma et al. 1998) with a correlated flux density of $\sim$ 300 mJy. The separation angle between the maser and the reference sources is 0.°73. Left-hand circular polarization signals were received for both S269 and J0613+1306, and digitally recorded onto magnetic tapes with the VERA-terminal system at the total data rate of 1024 Mbps. With 2-bit quantization, this data rate provides a total bandwidth of 256 MHz. The signals from the two sources were filtered with VERA Digital Filter (Iguchi et al. 2005) to obtain 1 IF (Intermediate Frequency) channel of 16 MHz for the S269 maser line and 15 IF channels of 16 MHz (240 MHz in total) for J0613+1306. Correlation processings were made with the Mitaka FX correlator. For the reference, which is a continuum source, the spectral resolution was 64 points per each 16 MHz channel, which corresponds to a velocity resolution of 3.4 km s^{-1}. For the maser source, the frequency and velocity resolutions were 15.625 kHz and 0.21 km s^{-1}, respectively.

Since the correlator's a priori delay model is not accurate enough for high-precision astrometry, recalculations of the precise delay were made after the correlation, and the correlated visibilities were corrected for any difference between the first (rather crude) a priori model and the second (more accurate) delay model. The delay recalculation code is based on the geodynamics models described in IERS convention 1996 (McCarthy 1996), and Earth orientation parameters (EOP) were taken from IERS bulletin B final values,[4] which currently provides the best estimates. Also, ionospheric delays were corrected based on the global ionosphere map (GIM), which is produced by the University of Bern every day.[5]

In the data analysis of each epoch, at first fringes were searched for the reference source, J0613+130. With a 240 MHz bandwidth and a typical system noise temperature of 200 K, the reference source, having a flux of $\sim$300 mJy, was easily detected within 1 minute integration, which is much shorter than the typical coherence time at 22 GHz (2 to 3 minutes). Since its position is accurately known, the fringe parameters of J0613+1306 were also used to calibrate the clock offset parameters (such as delay and delay-rate offset). The phase solutions for J0613+1306 were converted into the phase at the observed maser frequency, and applied to the visibilities of S269 together with the dual-beam phase calibration data. This dual-beam phase calibration data was taken in real-time during the observations, and are based on the correlation of artificial noise sources injected into two beams at each station (Kawaguchi et al. 2000). After those calibrations, the visibilities of the S269 masers were Fourier

[1] SIM: http://planetquest.jpl.nasa.gov/SIM/sim_index.cfm
[2] GAIA: http://sci.esa.int/science-e/www/area/index.cfm?fareaid=26
[3] JASMINE: http://www.jasmine-galaxy.org/index.html
[4] http://hpiers.obspm.fr/eop-pc/
[5] http://www.aiub.unibe.ch/ionosphere.html

transformed to synthesize images, and the positions of the brightness peaks were determined with respect to the reference spot. In some epochs (especially in summer), the qualities of phase-referenced maps were not high due to residuals in tropospheric delay. To calibrate them, residual zenith delays were estimated as a constant offset that maximizes the coherence of the phase-referenced map. Typical residuals of zenith delay are 1 to 5 cm, but in the worst case (during the summer at Ishigaki-jima station) it was as large as 20 cm.

3. Results

The total-power spectrum of S269 taken on DOY 073 in 2005 is shown in figure 1a. Basically, it consists of a single feature at $V_{\rm LSR}$[6] of $\sim 19.6\,{\rm km\,s^{-1}}$ with a peak intensity of 480 Jy, being consistent with a previous single-dish monitoring study (Lekht 2000). This main feature was always bright and observable for all of the epochs presented here. Figure 1b is the maser spot map of the main feature around $V_{\rm LSR}$ of $\sim 19.6\,{\rm km\,s^{-1}}$ (for DOY 2006/073). Six maser spots were detected in the velocity range from 19.0 to 20.1 km s^{-1}, and these maser spots are aligned in the east-west direction on a scale of 0.4 mas. It is remarkable that the thickness of the feature (spots distribution in the north-south direction) is $\sim 50\,\mu$as, 10-times smaller than the width in the east-west direction. The maser distribution also shows a velocity gradient from east to west. This kind of structure is rather unusual for H_2O masers in star-forming regions (which mostly show a bipolar structure with discrete blue/red-shifted clusters of maser spots) but, instead, similar to those of CH_3OH (methanol) masers at 6.7 GHz and 12.2 GHz in terms of the spot distribution as well as the velocity width (e.g., Minner et al. 2000). Note that the positions in figure 1b are the residuals to the tracking center positions of the maser and the reference sources, which were taken to be $(\alpha, \delta) = (06^{\rm h}14^{\rm m}37\overset{\rm s}{.}08, +13^{\rm d}49'36\overset{''}{.}7)$ for S269, and $(06^{\rm h}13^{\rm m}57\overset{\rm s}{.}692764, +13^{\rm d}06'45\overset{''}{.}40116)$ for J0613+1306, both in the J2000 coordinates. Thus, the absolute position of the brightest 19.6 km s^{-1} spot at DOY 073 of 2005 were obtained as $(06^{\rm h}14^{\rm m}37\overset{\rm s}{.}07933, +13^{\rm d}49'36\overset{''}{.}6945)$ with an uncertainty of 1 mas, which mainly comes from the uncertainty of the absolute position of the reference source, J0613+1306. The absolute position of the maser feature shown in figure 1b agrees well with the position of S269 IRS2w, which is the most luminous infrared source in the S269 regions (Jiang et al. 2003).

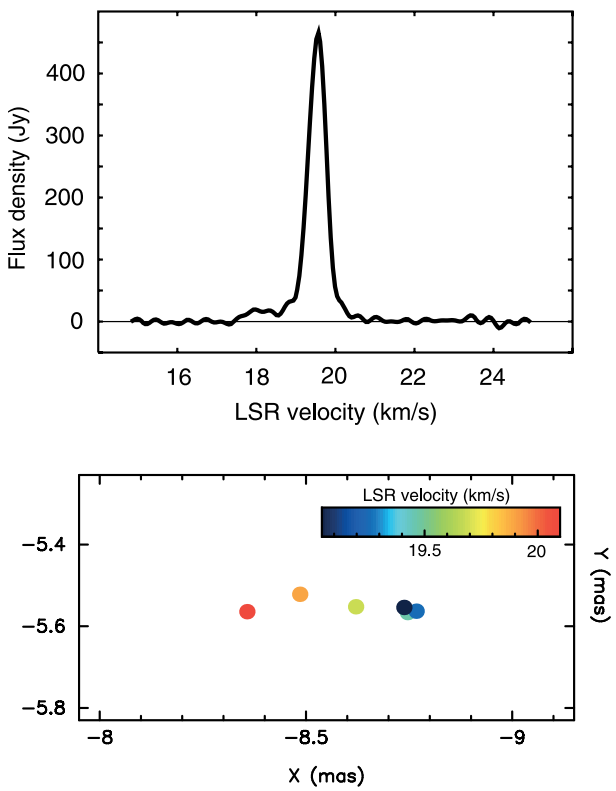

Fig. 1. (a, top) Auto-correlation spectrum of S269 H_2O maser emissions taken on DOY 073 in 2005. (b, bottom) maser spot distribution obtained with VERA on DOY 073 in 2005. The coordinates are with respect to the tracking center position, which is $(06^{\rm h}14^{\rm m}37\overset{\rm s}{.}08, +13^{\rm d}49'36\overset{''}{.}7)$ in J2000.0.

Figure 2 shows the positional variations of the brightest maser spot in the X ($\equiv \cos\delta\Delta\alpha$, east-west offset) and Y ($\equiv \Delta\delta$, north-south offset) directions for a monitoring span of 1 yr. As can be clearly seen from the plot (especially in X direction), the positions show systematic sinusoidal modulation with a period of 1 yr. The phase of the observed sinusoidal curve (i.e., the peak date) perfectly matches with that of the expected parallax curve for S269, ensuring that the modulation certainly originates from the parallax of S269. In figure 2, the error bars were estimated as the standard deviation from the best-fit with parallax plus linear proper motions. This error estimate was made because it is difficult to predict the observational error in VLBI astrometry; the error depends on many factors, such as the residual phase in phase-referencing, the error in zenith delay of the troposphere and the ionosphere, and the error in calibration of the instrumental offset, and so on, and is hardly predictable. The estimated error bars are 25 μas for X and 75 μas for Y. We note that the error in Y is three-times larger than that in X. This can be explained if one assumes that the majority of the error comes from the uncertainty in the tropospheric zenith delay, since the tropospheric delay changes the apparent elevations of the source. A detailed consideration of the error is discussed in the next section. For our parallax measurements, in this paper we consider only the X component, because the Y direction error is large, and also because S269 is near the ecliptic and the parallax ellipse is highly elongated in the X direction, making the contribution of Y to the parallax determination smaller. Here, we use the brightest three spots at the radial velocity from 19.4 to 19.8 km s^{-1}, including the brightest one at 19.6 km s^{-1} to ensure a high signal-to-noise ratio; as can be clearly seen from figure 1, the H_2O maser spectrum is sharply peaked at 19.6 km s^{-1}, and the maser intensity becomes weak at off-peak radial velocities. Least-squares fits were made to positions of the three maser spot, with parallax π as well as proper motions μ_X (east-west direction) and μ_Y

[6] The LSR velocity described here is in traditional definition using the Solar motion of (U, V, W) = (10, 15.4, 7.8) km s^{-1} (Kerr & Lynden-Bell 1986) for comparisons with previous observations.

Table 1. The best-fit values of parallax π and proper motions μ_X and μ_Y for the three brightest spots.

X (mas)	Y (mas)	$V_{\rm LSR}$	π (mas)	μ_X (mas/yr)	μ_Y (mas/yr)
−8.183	−5.571	19.8	0.208±0.030	−0.425±0.032	−0.123±0.076
−8.365	−5.591	19.6	0.199±0.012	−0.388±0.014	−0.118±0.071
−8.427	−5.602	19.3	0.176±0.012	−0.457±0.015	−0.123±0.072
mean			0.189±0.008	−0.422±0.010	−0.121±0.042

The last row gives the values obtained by weighted mean. Note that positions X and Y are those at the first epoch (DOY 323 in 2004) with respect to the tracking center position of S269, which was taken to be ($06^{\rm h}14^{\rm m}37\overset{\rm s}{.}08$, $+13^{\rm d}49'36\overset{''}{.}7$) in J2000.0.

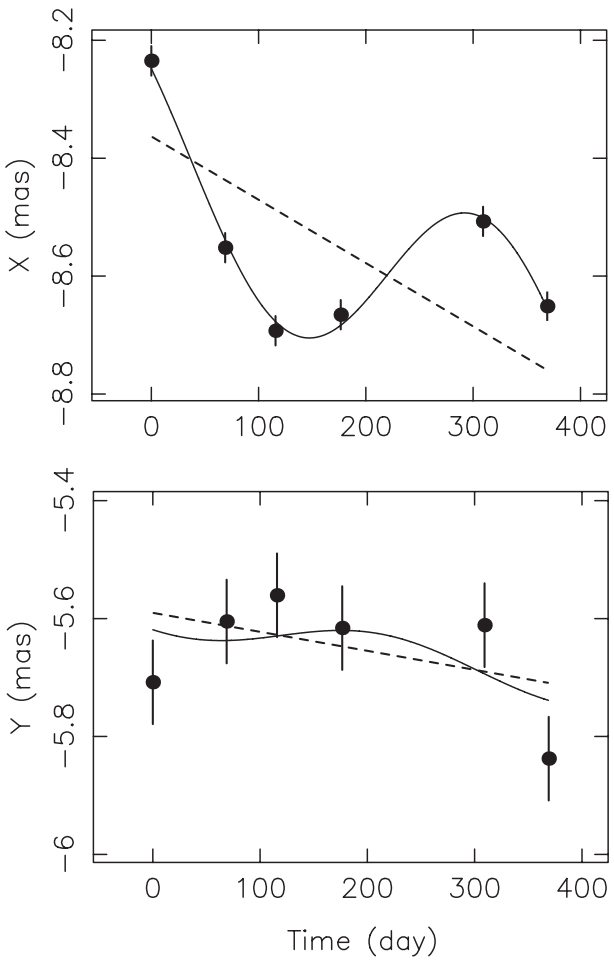

Fig. 2. Positional variations of the brightest maser spot at $V_{\rm LSR} = 19.6\,{\rm km}^{-1}$. Top is for X (east-west) direction and bottom is for Y (north-south) direction. The time origin is the first epoch of our observations, which is DOY 323 in 2004. The solid curves are best-fit results with parallax and proper motions, and the dashed lines show the best-fit proper motions.

(north-south direction). Table 1 summarizes the best-fit results. As can be seen in table 1, independent analyses for the three spots give results consistent with each other, from 176 μas to 208 μas. To obtain the best estimate of the parallax, π, we took a weighted mean of the parallaxes, yielding a parallax of S269 as 189 ± 8 μas, where the error bar is estimated to be $\sigma^2 = 1/\sum(1/\sigma_i^2)$. This corresponds to a source distance of $5.28^{+0.24}_{-0.22}$ kpc. This is the smallest parallax ever measured to date, demonstrating the high capability of VERA to perform Galactic-scale astrometry. The distance to S269 is found to be slightly larger than previous estimates, which claimed a distance of ∼4 kpc (Moffat et al. 1979).

From the fitting results in table 1, the weighted means of the proper motions were obtained as $(\mu_X, \mu_Y) = (-0.422 \pm 0.010, -0.121 \pm 0.042)$ mas yr^{-1}, respectively. To convert these observed (heliocentric) proper motions to the ones with respect to LSR, we used the solar motion based on the HIPPARCOS satellite data (Dehnen & Binney 1998), which is $(U, V, W) = (10.0, 5.25, 7.17)$ km s^{-1}. Using the galactic coordinates of S269 $(l, b) = (196\overset{\circ}{.}45, -1\overset{\circ}{.}96)$ and the Galactic plane's position angle of 151.51° there, one can calculate the proper motion projected to the direction of l and b as $(\mu_l, \mu_b) = (-0.184 \pm 0.032, -0.149 \pm 0.029)$ mas yr^{-1}. Given the source distance of 5.28 kpc, these proper motions correspond to a velocity vector of $(v_l, v_b) = (-4.60 \pm 0.81, -3.72 \pm 0.72)$ km s^{-1}, respectively. These velocity components are remarkably small compared to the rotation speed of the Galaxy, which is on the order of ~ 200 km s^{-1}. Given that S269 is located in the anti-center region, the small value of v_l indicates that the Galactic rotation velocities at the Sun and at S269 are close to each other, and the proper motions were cancelled out in our relative proper-motion measurements. A detailed discussion of the Galactic rotation velocity is given in the next section.

4. Discussion

4.1. Sources of Astrometric Error

As described in the previous section, the astrometric errors estimated from the fitting deviations are 25 μas for X and 75 μas for Y. These can be explained if the dominant error source is the uncertainty in the tropospheric zenith delay. For instance, if we take a typical uncertainty of 3 cm for the tropospheric zenith delay, then it causes a path-length difference of 0.4 mm (= 30 mm × 0°.7 / 57°.3/rad, where 0°.7 is the separation angle between S269 and the reference source) between the two sources. This uncertainty in the path-length difference roughly corresponds to 40 μas (= 0.4 mm / 2.3×10^9 mm, where 2.3×10^9 mm is the maximum baseline length of the VERA array). In practice, observations are not done toward the zenith, but sources are at a lower elevation angle (EL). Because our observations were usually made for an elevation angle larger than 20°, the effect

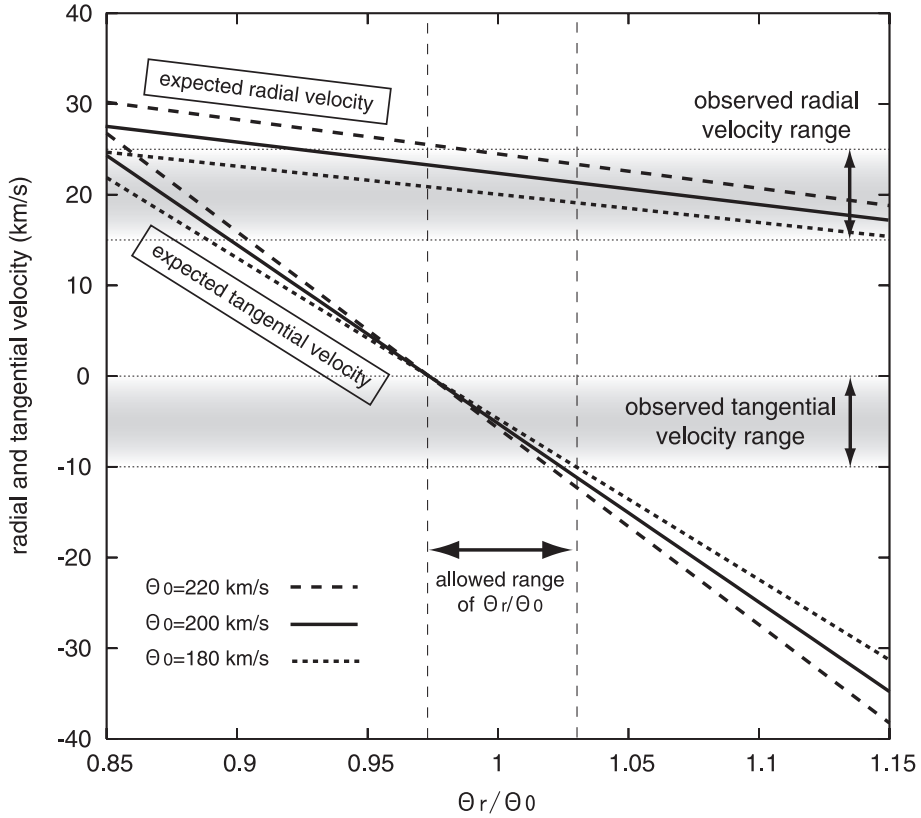

Fig. 3. Plot of the radial velocity, v_r, and tangential velocity, v_l, with respect to LSR as a function of the rotation velocity ratio, $\theta = \Theta/\Theta_0$. The observed value of $v_l (= -5 \pm 5)$ is consistent with the rotation velocity ratio of $\theta = 1.00 \pm 0.03$, showing that the rotation velocity is the same at the position of S269 and at the Sun. Note that $v_r (= 20 \pm 5)$ can be explained consistently with $\theta = 1.00 \pm 0.03$.

of the zenith delay error was multiplied by a factor of 1 (corresponding to $EL = 90°$) to ~ 3 ($EL = 20°$), depending on the source elevation. If this factor is taken into account, one can expect an astrometric error of 40 to 120 μas, depending on the EL distribution; the astrometric error in Y, obtained above (75 μas), is certainly in this possible range. On the other hand, the astrometric error in the X direction can be suppressed for two reasons: first, the source pair considered here has a smaller separation in the X direction than in the Y direction and, second, the observational track in each epoch is roughly symmetric with respect to the meridian transit (i.e., each epoch has nearly same track before and after the transit). This symmetry can help to reduce the astrometric error in the X direction caused by the tropospheric zenith delay offset.

Other possible sources of astrometric error are those in station positions, the delay model, and the ionosphere. Currently, VERA station positions are determined with an accuracy of ~ 3 mm based on geodetic observations at S/X (2/8 GHz) bands carried out every two weeks. Also, our delay calculation code was compared with CALC[7] developed by the NASA/GSFC VLBI group, which is the international standard of delay models. It turned out that the difference between the two codes is less than 2 mm. Therefore, these errors are smaller than that of the zenith delay by an order of magnitude. Regarding the ionosphere, its contribution is small at 22 GHz, and corrections with the GPS-based Global Ionosphere Map (GIM), provided by University of Bern, are precise enough for 10 μas astrometry. We note that the trend of the larger error in the Y direction was also found in other observations of VERA. Therefore, the larger error in Y is not a special phenomenon of only the S269 observations, but, rather, is common to all VERA observations, and is most likely to originate from the tropospheric zenith delay error.

4.2. *Constraint on Galactic Rotation*

Here, we use the proper motions and parallax obtained in the previous section to constrain the Galactic rotation velocity at the position of S269. First, the small proper motion perpendicular to the Galactic plane ($v_b = -3.72 \pm 0.72$ km s^{-1}) indicates that S269 basically partakes in galactic rotation, and also that the H_2O maser proper motions truly reflect the systemic motion of S269. Radial velocity measurements support the latter idea; while the maser emission is peaked at 19.6 km $^{-1}$, the peak velocity of HII region observed with SII lines is 16.5 km s^{-1}, and the systemic velocity of the associated molecular cloud observed in CO is 17.7 km s^{-1} (Godbout et al. 1997), which agrees well with the maser radial velocity within 3 km s^{-1}. Therefore, from the radial velocity as well as the proper motions perpendicular to the Galactic plane, one can expect that the peculiar velocity of the maser source with respect to pure Galactic rotation is as small as ~ 5 km s^{-1}.

[7] http://gemini.gsfc.nasa.gov/solve/

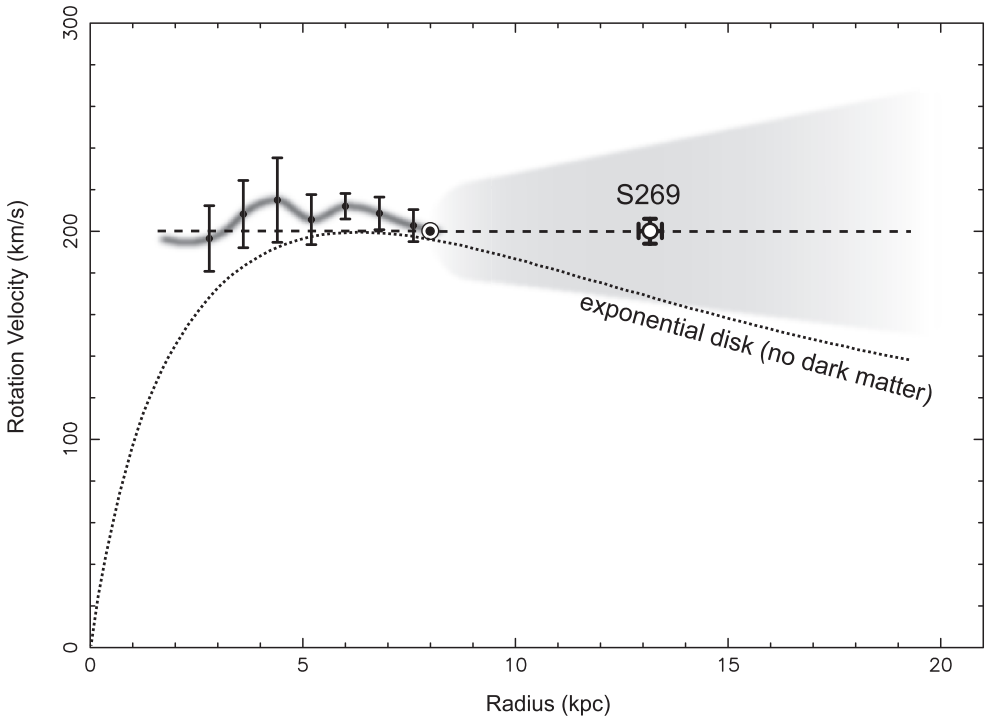

Fig. 4. Rotation curve of the Milky Way Galaxy obtained in previous studies together with our result for S269 using Galactic constants of $R_0 = 8$ kpc and $\Theta_0 = 200$ km $^{-1}$. The dashed line is the flat rotation curve with $\Theta = 200$ km^{-1}; the shadowed area shows the possible range of outer rotation curves considered in previous studies (Honma & Sofue 1997). Points at $R \leq 8$ kpc are inner rotation curves determined from the tangential velocities of Galactic HI gases (Honma & Sofue 1997), with a smoothed fit (thick curve). The dotted curve is the rotation curve for an exponential disk, corresponding to a constant mass-to-light ratio disk without dark matter. A discrepancy between the observed point for S269 and the exponential disk is evident, demonstrating the existence of a large amount of dark matter in the outer region of the Galaxy.

From this fact one can expect that the proper motion in the l direction (v_l) basically reflects the difference of the galactic rotation velocities at the position of S269 and at the Sun, and also that one can constrain the outer rotation velocity at the position of S269. In fact, S269 is located near to the galactic anti-center region ($l = 196.^\circ45$), and thus the lack of a large proper motion in the l direction indicates that the galactic rotation speed there is close to that at the Sun. If a source is on perfect Galactic rotation, the radial and tangential velocities with respect to LSR observers can be written as

$$v_r = \left(\frac{\Theta}{R} - \frac{\Theta_0}{R_0}\right) R_0 \sin l, \tag{1}$$

$$v_l = \left(\frac{\Theta}{R} - \frac{\Theta_0}{R_0}\right) R_0 \cos l - \frac{\Theta}{R} D. \tag{2}$$

For the component perpendicular to the Galaxy plane, obviously $v_b = 0$. These equations relate the observed velocities to the rotation velocity at the source (Θ) through the Galactic constants, R_0 and Θ_0. Figure 3 shows a plot of the expected v_r and v_l for S269 as a function of $\theta \equiv \Theta/\Theta_0$ (rather than Θ for seeing the difference of the rotation velocities at S269 and the Sun). Here, the Galactic constant, R_0, is assumed to be 8.0($\pm$0.5) kpc (Reid 1993), and three cases of Θ_0, 180, 200, and 220 km s^{-1} are considered as recent determinations of Θ_0 still vary substantially (Olling & Merrifield 1998; Miyamoto & Zhu 1998; Reid & Brunthaler 2004). As can be seen in figure 3, the tangential velocity, v_l, has a strong dependence on θ, and thus the observed v_l can be used to constrain the rotation velocity. Considering that the velocity component perpendicular to the Galactic plane is 3.7 km s^{-1}, and that the radial velocity differences between the maser and other lines (such as CO and SII) are also ~ 3 km s^{-1}, here we can safely assume the possible range of the true tangential velocity to be $v_l = -5 \pm 5$ km s^{-1}, and that of the true radial velocity is $v_r = 20 \pm 5$ km s^{-1}.[8] From figure 3, this tangential velocity range is obtained if θ lies between 0.97 and 1.03. Therefore, at the position of S269, θ should be 1.00 ± 0.03, i.e., the rotation velocity at the S269 (Θ) must be the same as Θ_0 within the 3% level. This is the strongest constraint of the rotation velocity in the outer galaxy ever obtained. Note that the same argument is possible based on the radial velocity, v_r, but the constraint is not as strong as that from the tangential velocity, because the gradient of $v_r(\theta)$ plot is much shallower. However, we note that the radial velocity, $v_r = 20 \pm 5$ km s^{-1}, can be consistently explained by a rotation velocity ratio of $\theta \sim 1$.

In previous studies, the Galactic rotation curve had an uncertainty of up to 100 km s^{-1} in the outer region if one included the strong dependence on Galactic constants, Θ_0 (Honma & Sofue 1997). This situation is summarized in

[8] Note that the radial velocity considered here is slightly different from the traditionally-defined $V_{\rm LSR}$ since the Solar motion considered here is the one recently obtained from HIPPARCOS data (Dehnen & Binney 1998). However, the difference in $V_{\rm LSR}$ and v_r is not significant, being 3.3 km $^{-1}$ for S269.

figure 4, showing the area of uncertainty in previous studies. The point for S269 determined in this study is also shown in figure 4. The coincidence of the rotation velocities at the Sun and S269 simply indicates that the rotation curve there is basically flat, as was known for the rotation curves of other spiral galaxies (Rubin et al. 1980; Rubin 1983; Sofue & Rubin 2001). In disk galaxies like the Galaxy, the optical surface brightness obeys an exponential law, i.e., $I(r) = I_0 \exp(-r/h)$, where r is the radius and h is the disk scale length. Assuming that the surface brightness traces the mass density (i.e., constant Mass-to-Light ratio), one can calculate the rotation curve of the optical disk, assuming no dark matter (Freeman 1970). In figure 4, we also showed such a rotation curve for the Galaxy's disk, assuming a disk scale length of $h = 3$ kpc and a maximum rotation velocity of 200 km^{-1}. As can be seen from figure 4, such a rotation curve without dark matter was not completely ruled out previously. However, the rotation velocity measurement for S269 evidently shows the discrepancy between the observed rotation curve and that expected from the optical disk without dark matter, providing a strong confirmation for the existence of dark matter in the Galaxy's outer region. At the position of S269, the rotation curve of the exponential disk gives $V_{\rm exp} = 168$ km s^{-1}, while the astrometric measurement of S269 provides $V_{\rm obs} = 200$ km s^{-1}. In the case of a spherical mass distribution, the enclosed mass, M_r, within radius r is proportional to V^2, as M_r can be written as $M_R \approx rV^2/G$. The values of $V_{\rm exp}$ and $V_{\rm obs}$ obtained above give $(V_{\rm exp}/V_{\rm obs})^2 = 0.70$, and thus within the position of S269 at least $\sim 30\%$ of the enclosed mass must be composed of dark matter.

Although this study presents astrometric measurements for only one source, the present study demonstrates the high capability of VERA for studying Galactic rotation based on Galaxy-scale astrometry. During the next decade, VERA will continue astrometric observations of nearly one thousand Galactic maser sources, and will provide an accurate rotation curve over the whole Galaxy's disk as well as an accurate description of the dark-matter distribution of the Galaxy.

We are grateful to the referee, Prof. Karl Menten, for carefully reading the manuscript. One of the authors (MH) acknowledges financial support from grant-in-aid (No.16740120) from the Ministry of Education, Culture, Sports, Science and Technology (MEXT). The authors also would like to thank all the supporting staffs at Mizusawa VERA observatory for helping observations.

References

Brand, J., & Blitz, L. 1993, A&A, 275, 67
Clemens, D. P. 1985, ApJ, 295, 422
Dehnen, W., & Binney, J. 1998, MNRAS, 298, 387
Freeman, K. C. 1970, ApJ, 160, 811
Godbout, S., Joncas, G., Durand, D., & Arsenault, R. 1997, ApJ, 478, 271
Hachisuka, K., et al. 2006, ApJ, 645, 337
Honma, M., & Sofue, Y. 1997, PASJ, 49, 453
Honma, M., Kawaguchi, N., & Sasao, T. 2000, Proc. SPIE 4015, 624
Honma, M., et al. 2003, PASJ, 55, L57
Iguchi, S., Kurayama, T., Kawaguchi, N., & Kawakami, K. 2005, PASJ, 57, 259
Jiang, Z., et al. 2003, ApJ, 596, 1064
Kawaguchi, N., Sasao, T., & Manabe, S. 2000, Proc. SPIE 4015, 544
Kent, S. M. 1986, AJ, 91, 1301
Kent, S. M. 1987, AJ, 93, 816
Kerr, F. J., & Lynden-Bell, D. 1986, MNRAS, 221, 1023
Kobayashi, H., et al. 2003, ASP Conf. Ser., 306, 367
Kurayama, T., Sasao, T., & Kobayashi, H. 2005, ApJ, 627, L49
Lekht, E. E. 2000, A&AS, 141, 185
Ma, C., et al. 1998, AJ, 116, 516
McCarthy, D. D. 1996, IERS Technical Note, No.21
Merrifield, M. R. 1992, AJ, 103, 1552
Minner, V., Booth, R. S., & Conway, J. E. 2000, A&A, 362, 1093
Miyamoto, M., & Zhu, Z. 1998, AJ, 115, 1483
Moffat, A. F. J., Fitzgerald, M. P., & Jackson, P. D. 1979, A&AS, 38, 197
Olling, R. P., & Merrifield, M. R. 1998, MNRAS, 297, 943
Perryman, M. A. C., et al. 1997, A&A, 323, L49
Reid, M. J. 1993, ARA&A, 31, 345
Reid, M. J., & Brunthaler, A. 2004, ApJ, 616, 872
Rubin, V. C., Ford, W. K., Jr., & Thonnard, N. T. 1980, ApJ, 238, 471
Rubin, V. C. 1983, Science, 220, 1339
Sofue, Y., & Rubin, V. 2001, ARA&A, 39, 137
Xu, Y., Reid, M. J., Zheng, X. W., & Menten, K. M. 2006, Science, 311, 54